Cell Tissue Res (2000) 302:243–251
DOI 10.1007/s004410000224

REGULAR ARTICLE

**Amy M. Collinsworth · Carol E. Torgan
Suneel N. Nagda · Robert J. Rajalingam
William E. Kraus · George A. Truskey**

Orientation and length of mammalian skeletal myocytes in response to a unidirectional stretch

Received: 5 November 1999 / Accepted: 3 March 2000 / Published online: 10 October 2000

Abstract Effects of mechanical forces exerted on mammalian skeletal muscle cells during development were studied using an in vitro model to unidirectionally stretch cultured C2C12 cells grown on silastic membrane. Previous models to date have not studied these responses of the mammalian system specifically. The silastic membrane upon which these cells were grown exhibited linear strain behavior over the range of 3.6–14.6% strain, with a Poisson's ratio of approximately 0.5. To mimic murine in utero long bone growth, cell substrates were stretched at an average strain rate of 2.36%/day for 4 days or 1.77%/day for 6 days with an overall membrane strain of 9.5% and 10.6%, respectively. Both control and stretched fibers stained positively for the contractile protein, α-actinin, demonstrating muscle fiber development. An effect of stretch on orientation and length of myofibers was observed. At both strain rates, stretched fibers aligned at a smaller angle relative to the direction of stretch and were significantly longer compared to randomly oriented control fibers. There was no effect of duration of stretch on orientation or length, suggesting the cellular responses are independent of strain rate for the range tested. These results demonstrate that, under conditions simulating mammalian long bone growth, cultured myocytes respond to mechanical forces by lengthening and orienting along the direction of stretch.

This work was supported by NASA grants NAG-910, NIH-NRSA AR08231 and a predoctoral fellowship to A.M.C. (NIH NRSA 5T32 GM0855503). W.E.K. is an Established Investigator of the American Heart Association

A.M. Collinsworth · S.N. Nagda · R.J. Rajalingam
G.A. Truskey (✉)
Department of Biomedical Engineering,
Box 90281, Duke University, Durham, NC 27708-0281, USA
e-mail: gtruskey@acpub.duke.edu
Tel.: +1 919 660 5147, Fax: +1 919 684 4488

C.E. Torgan · W.E. Kraus
Department of Medicine, Duke University, Durham,
NC 27708, USA

Keywords Mammalian skeletal myocytes · Orientation · Mechanical stretch · Developmental model · Mechanotransduction · Skeletal muscle

Introduction

The development, function, and adaptation of skeletal muscle in vivo are influenced by neural, electrical, hormonal, and mechanical factors. Mechanical stimuli are thought to play a significant role in influencing skeletal muscle, as this tissue experiences several different types of loads. For example, continuous loading occurs during developmental long bone growth, and cyclic loading occurs during exercise and movement. The effects of mechanical unloading are seen with the atrophy of skeletal muscle after exposure to a low-gravity environment or long-term bed rest (Baldwin 1996).

One way to observe the effects of loading on skeletal muscle is by studying morphologic changes in loaded fibers, such as fiber orientation and length. The orientation of muscle fibers is critical to the function of the whole muscle, as the fiber angle relative to the direction of shortening affects force production (Gans and Gaunt 1991). Muscle fibers can be arranged parallel or pinnate to the long axis of the muscle. In pinnate muscles, fiber force transmitted to the tendon is reduced due to the fibers being oriented at an angle to the long axis of the muscle. However, a larger number of fibers can be packed in a smaller cross-sectional area, resulting in an increase in the maximum force production of the muscle. In parallel muscles, the same amount of muscle tissue is arranged in longer fibers, which have a faster speed of shortening, but which also generate less power. Consequently, the architectural arrangement of muscle fibers within a muscle is one of the primary mechanisms used to determine functional specificity (Garrett and Best 1994).

In vitro, several cell types have been found to orient in response to mechanical stimuli, such as stretch. Cells have often been shown to align perpendicular to the axis

of stretch. For example, avian osteoblasts (Buckley et al. 1988), human endothelial cells (Shirinsky et al. 1989), cardiac myocytes (Terracio et al. 1988), smooth muscle cells (Mills et al. 1997) and even avian skeletal muscle cells (Vandenburgh 1988) all align perpendicular to the direction of cyclic mechanical stretch. Contrasting results such as no change in orientation in cardiac myocytes (Samuel and Vandenburgh 1990) and parallel alignment of smooth muscle cells grown in a 3D matrix (Kanda and Matsuda 1994) have also been reported, indicating that a large number of variables are involved in producing a specific response. The stretch pattern appears to be critical, as human endothelial cells align parallel to the direction of a manual stepwise stretch (Ives et al. 1986), and in response to a continuous unidirectional stretch, mammalian cardiac (Samuel and Vandenburgh 1990) and embryonic avian skeletal muscle cells (Vandenburgh and Karlisch 1989) align parallel to the axis of stretch.

Although responses of avian skeletal myocytes have been characterized, there is reason to believe that avian and mammalian cellular responses may be quite different (White and Esser 1989; Russell et al. 1992). In general, avian cell types tend to have a narrower range of responses, whereas mammalian cells can be manipulated (e.g., with electrical stimulation) to express a wide range of protein isoforms, demonstrating more plasticity than the avian cell types (Eisenburg and Salmons 1981). Thus to fully understand the responses of human skeletal muscle to physiologic, pathologic stimuli and various environmental stimuli (e.g., spaceflight), it is important to study mammalian tissues in a variety of experimental systems.

In vivo models present significant difficulties for the study of mechanical cellular signal transduction. Due to the simultaneous stimulation of the cell by other environmental factors in vivo, it is difficult to isolate the effects of mechanical stimulation alone. We have used a modified in vitro model described previously (Vandenburgh and Karlisch 1989) to mechanically stretch cells in an attempt to isolate the mechanical stimulus from other environmental stimuli and to study the effects of increased loading at the cellular level.

The objectives of this study were to test the hypotheses that (1) in response to a very slow unidirectional stretch, with rates in the range of in utero long bone growth in mice, mammalian muscle cells would begin to align in the primary direction of stretch, and (2) strain rate would affect the alignment of muscle fibers. There are several models available that impose an isotropic or nearly isotropic strain field (Andersen and Norton 1991; Belloli et al. 1991; Brighton et al. 1991; Schaffer et al. 1994). However, a biaxial strain field model, designed initially for avian cells (Vandenburgh and Karlisch 1989), was characterized and used to mimic in vivo mechanical forces imposed on mammalian skeletal muscle during development. This device was used to examine the effects of loading by qualitatively and quantitatively measuring the morphology of mammalian skeletal muscle cells in response to a unidirectional stretch. Morphology measurements included fiber length and the orientation of the fibers relative to the direction of stretch. Immunohistochemistry was used to visualize the fibers. In this study, a slow unidirectional stretch was found to significantly affect the orientation and length of the mammalian skeletal muscle fibers.

Materials and methods

Construction of the stretch device

The stretch device (30.5×38 cm) consisted of two sets of aluminum racks, each capable of holding a total of nine membrane wells. One rack was attached to a stepper motor (Model SLS, Hurst Manufacturing, Princeton, IN) via a linear actuator rod and was mounted on a translation stage (NewPort Klinger, Irvine, CA). The motor was connected to a Macintosh computer via a digital I/O connector (MacADIOS 8dio, GW Instruments, Somerville, MA). Programs written in C language were used to impose a slow, gradual stretch to the membrane wells in the attached rack. The other rack of wells was used for nonstretch controls. The entire stretch device was covered with a removable Plexiglas lid. The stretch device was sterilized using ethylene oxide gas. It was then allowed to air out for 1 week under a cell culture hood before use. During experiments, the device was placed in an incubator to keep cells at 37°C and 5% CO_2.

Stretching of the membrane wells

The strain behavior of the silastic membrane was characterized by measuring the movement of beads attached to a bare membrane well while it was being stretched. The cell culture wells (3.2×1.5 cm) were made of silastic membrane (Speciality Manufacturing Inc., Hemlock, MI) by gluing the ends with adhesive silicone (Type A, Nusil Technology, Carpinteria, CA), which resulted in a shape resembling a shoe box. After the silastic membrane was assembled into rectangular-shaped wells, 180- to 230-µm polystyrene ion exchange resin beads (IRA-93, Rohm and Haas Co., Philadelphia, PA) were attached to the membrane. To ensure that the beads would adhere to the silastic, they were mixed in 1 ml 2% pigskin gelatin (Sigma, St. Louis, MO) and allowed to incubate for 30 min. A thin layer of the bead mixture was then spread evenly over the membrane well. Excess gelatin was immediately removed, and the membrane was allowed to dry for 24 h.

Bead-coated membrane wells were assembled and placed in the stretch side of the device. Both the stepper motor and a CCD Cohu camera were separately connected to a Macintosh LC III computer. The camera was mounted vertically above the stretch device so that the central portion of the membrane was in the field of view. A specified rate of stretch was programmed, and images were taken of the same field of view using a Neotech Image Grabber at a designated time interval during the entire stretch. Imposed stretch was along the long axis of the wells.

Strain analysis

The movement of beads was analyzed using Ultimage software (GFTS Inc., Santa Rosa, CA), which resulted in a set of coordinates describing the location of each bead. These data were then used to calculate strain using analysis of deformation, which relates changes in the relative movement of beads to the strain. This method is based on the change in distance among a triad of three points (Fig. 1). The strain components are defined as (Fung 1965):

$$ds^2 - ds_o^2 = 2E_{ij}da_i da_j \quad (1)$$

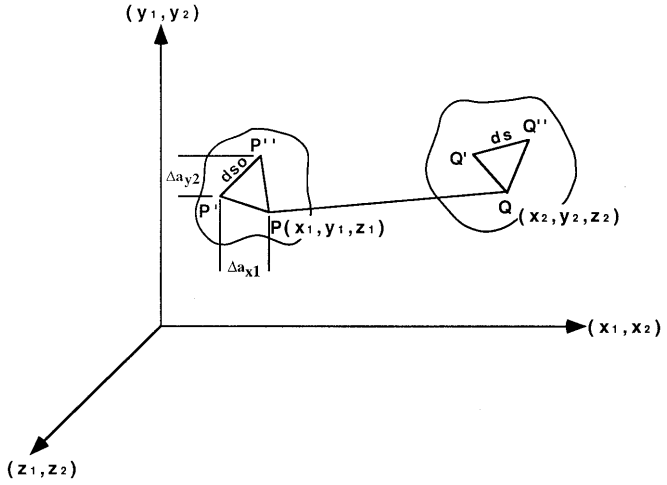

Fig. 1 Triad method often used to calculate deformation. Points P, P', and P'' represent an undeformed triad and Q, Q', and Q'' represent the deformed positions. The membrane was stretched in the *x*-direction (adapted from Fung 1993)

where ds and ds_o are the deformed and undeformed lengths, respectively, between two points, and da_i are the differences in coordinates of ds. The plane strain components (E_{xx}, E_{xy}, E_{yy}, where i and j have been replaced by x, the direction of imposed stretch, and y, the direction orthogonal to and in the same plane as x) can then be determined by measuring the deformation of a triad of beads (Fung 1965) and solving the system of equations from the expanded form of Eq. 1:

$$\left(\Delta s^2 - \Delta s_o^2\right)_k = 2\left(E_{xx}\Delta a_x \Delta a_x + 2E_{xy}\Delta a_x \Delta a_y + E_{yy}\Delta a_y \Delta a_y\right)_k, \quad k = 1 \text{ to } 3 \tag{2}$$

where k denotes each of the three pairs of beads in the triad. Using the plane strain components, the two principal strains were determined by solving the equation:

$$\left(E_{ij} - E\delta_{ij}\right)v_i = 0 \tag{3}$$

where v_i is the direction vector. Because the membrane was stretched in the x direction, the largest valued solution to Eq. 3 was defined as E_{xx}.

A propagation of error analysis was performed on the triad method. Strain is a function of 12 variables (see Eq. 2); therefore, the propagation of error equation is written as:

$$\sigma_{Exx} = \left(\sum_{k=1}^{3}\left(\frac{\partial E_{xx}}{\partial da_{x_k}}\right)^2\left(\sigma da_{x_k}\right)^2 + \left(\frac{\partial E_{xx}}{\partial da_{y_k}}\right)^2\left(\sigma da_{y_k}\right)^2 + \left(\frac{\partial E_{xx}}{\partial ds_k}\right)^2\left(\sigma ds_k\right)^2 + \left(\frac{\partial E_{xx}}{\partial ds_{o_k}}\right)^2\left(\sigma ds_{o_k}\right)^2 + \ldots\right)^{\frac{1}{2}} \tag{4}$$

where the standard deviation for a given length measurement (σda_{x_k}=σda_{y_k}) was one-half of a pixel. Mathematica software (Wolfram Research Inc., Champaign, IL) was used to solve for the derivatives of the strain matrix.

Skeletal muscle culture and stretch

The membrane wells were assembled into holders and the tension was adjusted so that the bottoms of the wells were flat. They were then coated with 100 µg/ml growth factor reduced Matrigel (GFR) (Becton Dickinson, Bedford, MA). Matrigel matrix, whose major components are laminin, collagen IV, entactin and heparan sulfate proteoglycan, supports myotube formation better than each component alone (Funanage et al. 1992; Lyles et al. 1992; Maley et al. 1995). However, GFR Matrigel was used, as regular Matrigel tends to delay the onset of myotube formation (Hartley and Yablonka-Reuveni 1990). Cells grown on membranes coated with GFR Matrigel were more developed, in terms of fiber length and diameter, than those grown on wells coated with a 2% gelatin substrate (Sigma, St. Louis, MO) (data not shown). Initially, cell density was varied to find the optimum plating density.

Murine C2C12 myoblasts (American Type Culture Collection, Rockville, MD), a subclone derived from a cell line that originated from normal adult C3H mouse leg muscle (Yaffe and Saxel 1977; Blau et al. 1985), were used. They were plated in GFR Matrigel-coated wells at a density of 7.5×10^4 cells/well in Dulbecco's modified Eagle's medium (DMEM) (GibcoBRL, Grand Island, NY) supplemented with 10% calf serum (HyClone Laboratories, Logan, UT), 0.5% chick embryo extract (GibcoBRL), and 0.5% gentamicin (GibcoBRL). At 80–90% confluency, the medium was removed and replaced with DMEM supplemented with 10% horse serum (Intergen, Purchase, NY) and gentamicin to promote differentiation (process referred to as shifting). Cells were fed daily. Over the subsequent several days, the individual myoblasts underwent differentiation and fusion into multinucleated myotubes. The day before the cells were shifted, stretching was initiated. The membranes were stretched an average rate of either 0.048±0.001 mm/h for 4 days or 0.036±0.002 mm/h for 6 days. These rates were chosen as they are representative of long bone growth rates during prenatal mouse development (Patton and Kaufman 1995). The average strain in the x-direction was 9.45±0.24% for the 4-day experiments and 10.63±0.60% for the 6-day experiments. Measurements recorded determined that the average strain rates were 2.36±0.07%/day and 1.77±0.23%/day, respectively. Because the deformation of the membrane was so small, the change in strain rate over the period of stretch was negligible, resulting in an essentially constant strain rate. Measurements of the magnitude of stretch were made with a resolution of 0.01 mm. Parallel sets of non-stretched control cells were grown in each experiment inside and outside the device. After the stretch program was complete, the medium was removed and the cells were fixed in 2% formaldehyde and permeabilized in 0.25% nonidet P-40. The cultures were then immunostained for the contractile protein, α-actinin (Sigma A-7811), in order to visualize the myotubes, using methods previously described (Rastinejad and Blau 1993; Torgan et al. 1996). Stained fibers were imaged using a Kodak Megaplus Camera, and a Power Macintosh 7100 computer with MAXXGrab application (Precision Digital Images Corporation, Redmond, WA). The average resolution of the images was 97 pixels/mm. Approximately 10–12 images were taken of each membrane well. Depending on final cell density, the number of fibers selected from an individual well ranged from 50 to 124. It was statistically determined that 50 fibers selected from each membrane were sufficient to produce an accurate representation of the population mean (data not shown). There did not appear to be any correlation between final confluency of the membrane and cell response. Fibers were not selected from the outermost area of the membrane, including edges along the length of the membrane and the very ends. Thus, approximately 75% of the surface area of the membrane was used for experimental analysis. Both the orientation of the fibers, which was defined as the angle of the selected fiber relative to the direction of stretch, and the length of the fibers were measured. These parameters were analyzed using NIH Image software (Bethesda, MD). An average for each well was calculated, then all wells in one group were pooled to obtain an average for each condition in one experiment. The percentage increase in fiber length was defined as the difference in final length between control and stretched fibers divided by the average length of fibers in the control group. Due to variability in fiber lengths between experiments, the data were compared in terms of normalized lengths. Each experiment was treated as a single data point and the average (n=4) for each duration of stretch was analyzed. Unstretched control fibers, grown in wells both inside and outside the device, were analyzed in each experiment.

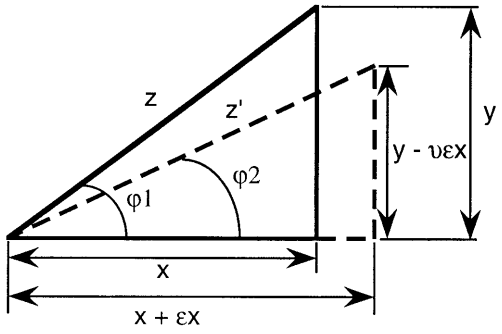

Fig. 2 Method to calculate passive orientation and length response of cells to 10% (ε) stretch in the *x*-direction. Poisson's ratio (υ) of the membrane is approximately 0.5

Calculation of passive deformation due to stretch

To give reference to the magnitude of the observed response of the cells, the deformation of the membrane due to stretch was calculated. This was done using simple geometry (Fig. 2). The equations describing the change in angle and length are as follows:

$$\tan\phi_2 = \frac{\tan\phi_1 - \upsilon\varepsilon}{1+\varepsilon} \tag{5}$$

$$z' = \frac{z(\sin\phi_1 - \upsilon\varepsilon\cos\phi_1)}{\sin\phi_2} \tag{6}$$

where z and z' are the undeformed and deformed distances between material points on the membrane, ϕ_1 and ϕ_2 are the initial and final orientations respectively, υ is the Poisson's ratio of the substrate material, and ε is the imposed strain. Depending on the number of focal contacts and the rate of migration, cells may or may not initially deform in a uniform manner similar to the membrane. In addition, the stretch is initiated several days before the myoblasts have formed tubes. It should be emphasized that the deformation is being made on single cells that have not yet fused to form multinucleated myotubes. However, if mature fibers were to passively deform with the membrane in response to stretch, the change in length and angle that would occur if a preexisting fiber were to be stretched 10% on the silastic membrane with a Poisson's ratio of 0.5, was calculated to be 3.3% and 4.3°, respectively.

Statistical analysis

All values are reported as the mean ± standard error unless otherwise stated. Lengths are reported in millimeters and angles are reported in degrees. To compare stretched and control fibers, if the averages of the inside control and outside control groups were found to be statistically the same, then stretched fibers were compared with the pooled control group. However, if control groups were found to be statistically different, stretched fibers were compared with control fibers grown inside the device only. Statistical significance between the effect of stretch (stretch versus no stretch) and the effect of rate of stretch (0.036 vs 0.048 mm/h) was calculated using two-way analysis of variance. Statistical significance between passive deformation and cellular response was calculated using the paired Student's *t*-test. Significance was defined as $P<0.05$.

Results

Characterization of the membrane substrate

Using the stretch device and imaging methods outlined above, the strain distribution along the membrane was calculated in response to a stretch imposed in the *x*-direction. Using triads of beads, the average strain in the *x*-direction was calculated to be the same as the imposed strain (Table 1). Placing the membrane well under tension so that the bottom of the well was flat, the strain distribution along the length of the membrane was found to be uniform in the range of 3.6–14.6% strain. For a 10% strain in the *x*-direction, there was a 5% narrowing in the transverse direction, yielding a Poisson's ratio of 0.5 for the silastic membrane. This results in a larger tensile force on the cells in the direction of stretch and a smaller shortening or compressive force on the cells in the transverse direction. Other models (Ives et al. 1986; Terracio et al. 1988; Vandenburgh and Karlisch 1989; Neidlinger-Wilke et al. 1994) which impose a unidirectional stretch likely apply this compressive force, and consequently exhibit a biaxial strain field. While the exact deformation exerted on the cells is not known, it has been shown that the deformation of endothelial cells grown on a silastic membrane is approximately the same magnitude as the substrate strain (Caille et al. 1998). From a zero deformation experiment, the accuracy with which strain could be measured was found to be 0.9% at a 95% confidence level.

Table 1 Characterization of membrane: principal strains

Location	Center	Edge
Applied strain	0.049	0.036
Exx±SD	0.047±0.006	0.036±0.008
Eyy±SD	0.022±0.003	0.019±0.006
Poisson's ratio±SD	0.47±0.09	0.53±0.08

Cell stretch experiments

This study consisted of eight separate stretch experiments, four of which imposed a 4-day stretch on the cells and four of which imposed a 6-day stretch. An individual experiment contained 1–14 separate wells at each condition (stretched or control). At least 50 fibers were selected from each well analyzed, to yield the average of that well. For both angle and length, the variation among experiments was smaller than the variation within a given experiment. Each experiment was thus treated as a single data point. The data represent the average of the four experiments at each strain rate.

The mammalian skeletal muscle cells developed into myofibers on the silastic membrane wells in the stretch device. Skeletal muscle development includes differentiation and fusion of myoblasts. Differentiation involves cessation of DNA synthesis and initiation of required transcription events, and sometimes includes cytoplasmic fusion. The fusion of myoblasts is an active process that involves close proximity of the cells, contact of the lipid bilayers and finally the fusion itself (Franzini-Armstrong and Fischman 1994). As fusion and elongation continue, the result is the formation of long, multinucleated cells

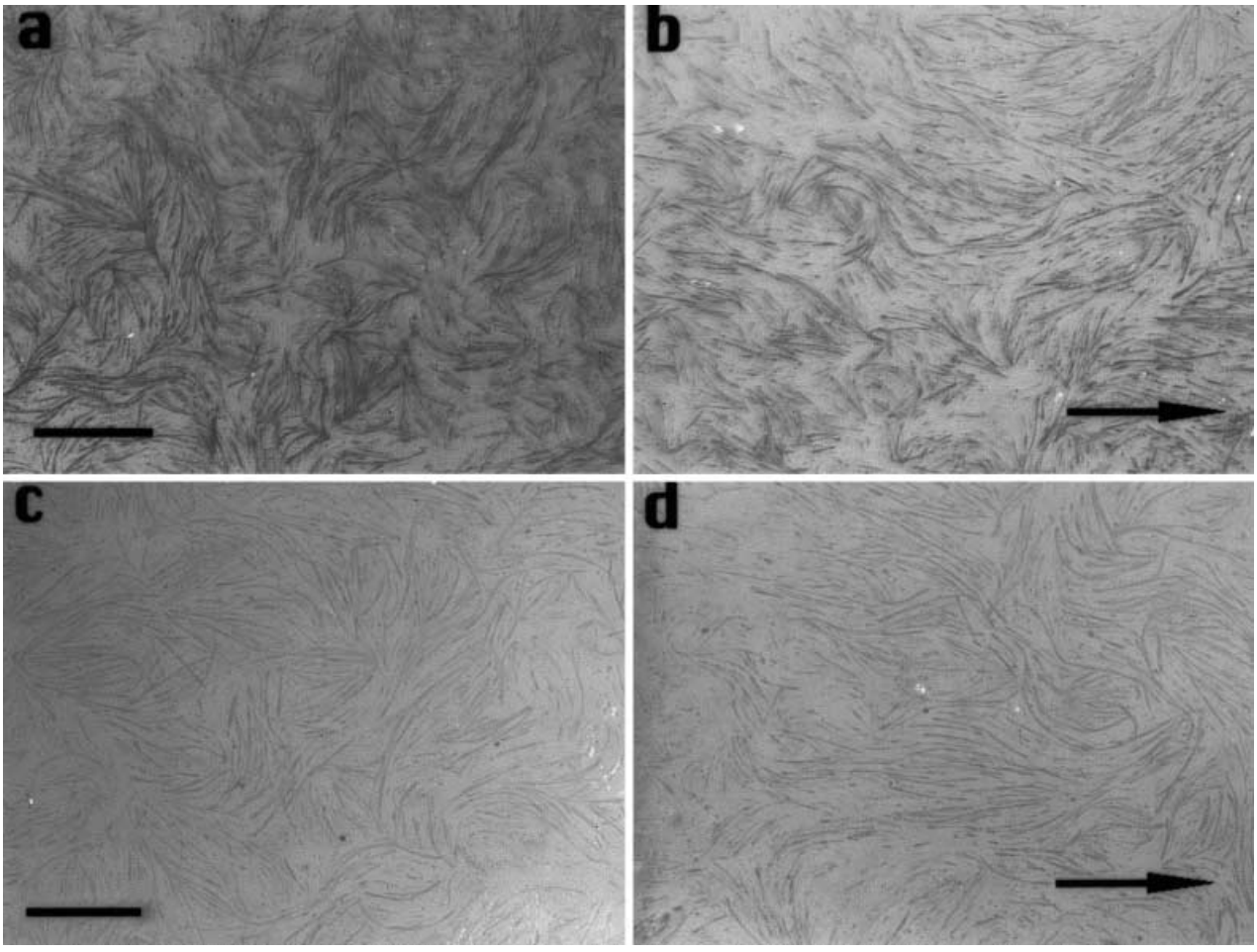

Fig. 3a–d Response of mammalian skeletal muscle fibers stretched for **b** 4 and **d** 6 days after shifting to 10% horse serum medium, along with their respective unstretched controls **(a)** and **(c)**. Fibers were stained for the contractile protein, α-actinin. *Scale bars* 1.0 mm

called myotubes. Myotubes are visible approximately 3 days following shifting, after which myotubes continue to grow. Consequently, during the first few days of experiments, stretch was imposed on actively fusing myoblasts. Staining of the fibers for the contractile protein, α-actinin, after 4 or 6 days of stretch (Fig. 3), confirmed that the cells were differentiating, as this muscle-specific protein, located in the *Z*-line of the sarcomeres, is not expressed until fusion of the myoblasts occurs (Endo and Masaki 1984). Before stretch, cells appeared in clusters of aligned cells, but the clusters did not preferentially align in any one direction, resulting in a randomly oriented cell population. However, after stretch, the majority of the cells were in clusters aligned with the direction of stretch.

Each experiment resulted in distributions describing the angles of orientation and the lengths of the fibers. The representative histograms shown in Fig. 4 reveal that there were changes in the morphology of the cell population after mechanical stretch. Data in Fig. 4 describe a single experiment in which cells were stretched for 6 days following shifting. Histograms describing individual 4- and 6-day experiments were similar. The angle distributions were skewed toward lower angles after stretch compared to the control distributions, indicating the tendency of the fibers to orient along the direction of stretch. The change in shape of the distributions showed a random angle of orientation initially, indicating no preferred orientation (Fig. 4a), but a biased orientation toward a smaller angle after stretch (Fig. 4b). In the length distributions, often there was a shift to a longer fiber mean, but the minimum and maximum were similar (Fig. 4c,d). The shapes of the length distributions generally remained the same between stretched and control fibers, indicating the effect of stretch upon fiber length was constant throughout the population.

A two-way analysis of variance (stretch versus rate) revealed that there was an effect of stretch on both the orientation ($P<0.002$) and percentage increase in length ($P<0.03$). All experiments showed a decrease in angle after stretching. The average orientation angles of stretched fibers were significantly smaller (34.78±0.8°, 36.54±2.19°) than the average angles of control fibers (40.79±0.6°, 43.08±1.74°) at both 4 and 6 days respectively, demonstrating that the fibers subjected to a unidirectional stretch aligned along the long axis of stretch (Fig. 5). Because the lengths of fibers were variable from

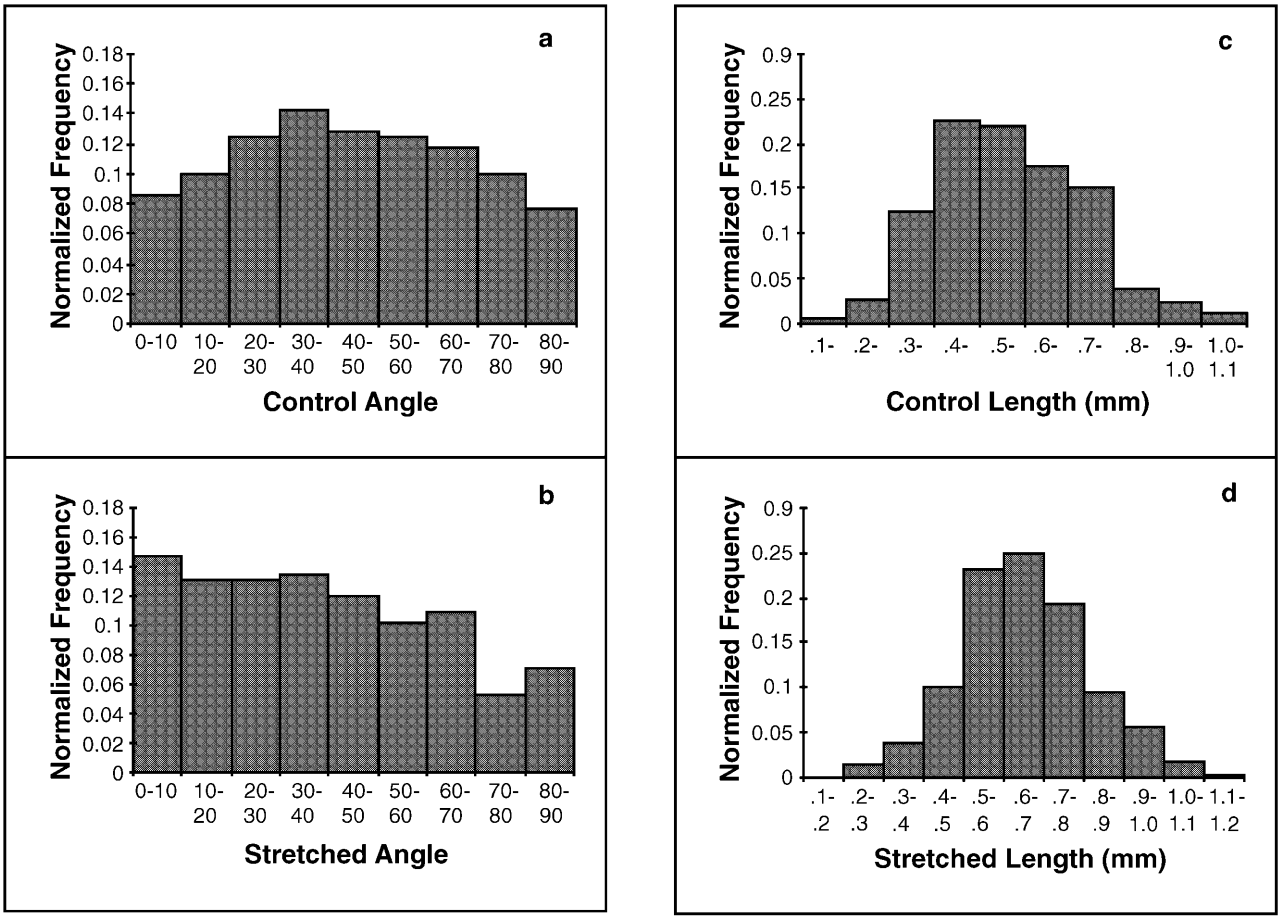

Fig. 4a–d Histograms of **a,b** the orientation response and **c,d** the length response of control and stretched fibers from an individual experiment in which cells were stretched for 6 days after day of shifting. The means±SE are **a** 44.27±1.18°(control), **b** 38.85± 1.50° (stretch), **c** 0.57±0.01 mm (control), and **d** 0.66±0.01 mm (stretch)

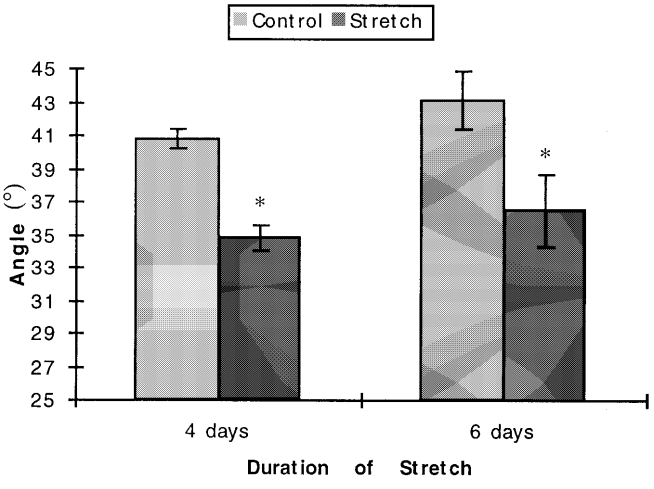

Fig. 5 Orientation of mammalian skeletal muscle in response to 4 or 6 days of stretch at a strain rate of 2.36±0.07% and 1.77±0.23%/day, respectively (n=4). *Asterisks* indicate significance, P<0.05. Standard error bars are shown

experiment to experiment, normalization of the data permitted useful comparisons. The average percentage increase in length of the fibers after stretch was 10.8±7.3% for the 4-day and 10.7±4.5% for the 6-day experiments (Fig. 6).

Analysis of variance showed no effect due to rate of stretch on myofiber orientation (P<0.16) or length (P<0.99). The magnitudes of strain in the two sets of experiments were the same, but the strain rates were different. Therefore, the orientation and percentage increase in length of the myofibers were independent of strain rate over the range tested. There were no interaction effects between stretch and time of stretch on either cellular responses measured.

Discussion

Mechanical forces influence physical and morphologic changes (Vandenburgh 1982; Galler 1994) as well as biochemical changes in skeletal muscle (Goldspink et al. 1991; Alway et al. 1995; Vandenburgh et al. 1995; Baldwin 1996; Brownson and Loughna 1996). The in vitro model we used allowed us to isolate and study the effects of mechanical stretch on mammalian skeletal muscle cells. We found that these cells respond to mechanical forces in vitro by aligning along the direction of

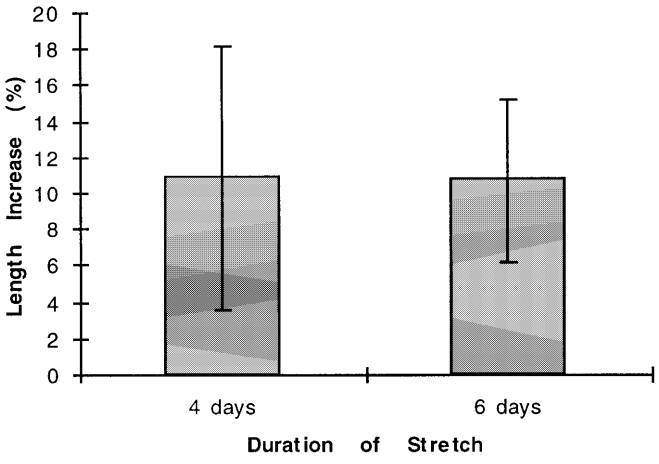

Fig. 6 Percentage increase in length of mammalian skeletal muscle in response to 4 or 6 days of stretch at a strain rate of 2.36±0.07% and 1.77±0.23%/day, respectively (n=4). Standard error bars are shown

stretch under conditions simulating long bone growth, and that stimulated muscle fibers were longer than control fibers. There was no effect of strain rate on the cells' orientation and length responses.

These results obtained in our mammalian model are similar, but not identical, to those previously described in avian models (Vandenburgh and Karlisch 1989). Although continuous stretch caused alignment and lengthening of muscle cells in both models (Vandenburgh and Karlisch 1989), length increases in the mammalian cells were not as great as the two- to fourfold increase Vandenburgh reported using avian cells. Orientation responses were similar in that the average angle of stretched fibers reported here is close to the nonstringent ±30° range around the stretch axis that Vandenburgh uses for parallel orientation criteria. They are not as close to his stringent ±10° criteria (Samuel and Vandenburgh 1990). Several differences in experimental design might account for the magnitude of responses observed in the various experiments. It is important to note that the rate of stretch used in Vandenburgh's study (0.35 mm/h) was the rate of avian bone elongation, and is approximately 10 times faster than the rate of mouse bone elongation used here. The use of an adult cell line may have inherent differences in satellite cell capacity, causing a diminished or delayed increase in myoblast fusion. Differences in the length response may also be simply due to the difference in species of cells.

The orientation response of the stretched fibers supports the proposition of a large body of literature that mechanical loading directly affects cellular processes. Numerous studies have demonstrated the plastic nature of striated muscle cells in their ability to adapt to stress. After only 2–4 weeks, pressure overload in cat hearts results in hypertrophy and increased microtubule density in the overloaded cardiocytes (Tsutsui et al. 1994; Tagawa et al. 1996). Chronic static stretch in rabbit limbs will also elicit a hypertrophy response from skeletal muscle cells (Goldspink et al. 1991). Other in vivo studies by Goldspink demonstrate that rabbit skeletal muscle cells will adapt after only 4 days (Williams et al. 1986), and cat soleus will adapt after 4 weeks (Tabary et al. 1972) to a chronic static stretch by increasing the number of sarcomeres in series, implying an increase in fiber length. The results presented here show that mammalian skeletal muscle cells in vitro also respond to mechanical loading by lengthening. Thus our results demonstrate that mammalian skeletal muscle cells loaded in vitro respond similarly to mechanically loaded muscle in vivo. The orientation of myocytes may be a critical step in skeletal muscle's ability to organize into parallel arrays of fibers aligned with the long axis of the muscle belly. Our findings suggest that the mechanical stimulus, without neural, hormonal or electrical influences, can affect the orientation of mammalian skeletal muscle in vivo. The orientation responses reported here concur with other in vitro studies investigating the effects of mechanical loading. Human endothelial cells (Ives et al. 1986) and avian skeletal muscle cells (Vandenburgh 1988; Vandenburgh and Karlisch 1989) orient parallel to the long axis of a continuous stretch.

The strain field to which the cells responded was uniform in the range of 3.6–14.6% stretch. The Poisson ratio of the substrate is 0.5, which results in a non-zero strain on the cells in the transverse direction. The cells are simultaneously exposed to the strains in both directions. It is difficult to say how important the transverse component is in producing the results, but it is known from the lengthening and contracting of skeletal muscle along its long axis that a biaxial strain is more relevant to skeletal muscle than a equibiaxial strain, which would be more likely to occur in a smooth muscle or endothelial cell environment. Alternatively, a constant volume approximation often used with muscle, implying a purely unidirectional strain, is also not physiologically relevant as there must be some transverse compression with elongation. We conclude therefore that a transverse strain imposed on the muscle cells provides a physiologically realistic component to the mechanical loading.

The orientation and increase in fiber length was statistically the same for fibers that were stretched for either 4 or 6 days. Since the two stretch conditions differed in strain rates but not strain magnitude, these data suggest that the signals responsible for the observed changes are strain rate independent within the range of rates tested. While a different strain rate may elicit a different response by the cells, we chose to remain within the physiological range of long bone growth in mice while testing the dependence on strain rate. Independence of strain rate would suggest that mouse skeletal muscle will develop in oriented parallel arrays while being stimulated at various strain rates within this range.

The applied strain used in these experiments induced certain cellular responses, suggesting these skeletal muscle cell responses are dependent on strain magnitude. Strain-dependent responses are possible as the orientation of smooth muscle cells (Mills et al. 1997) and cardi-

ac myocytes (Samuel and Vandenburgh 1990) are strain dependent. The amount of strain the cells experienced may not be the exact magnitude of the imposed strain on the membrane. However, we do know that the cells are deformed due to the fact that they are attachment dependent and no evidence of cell detachment was present. In addition, it has been shown in endothelial cells that the deformation of the cells closely follows that of the membrane substrate (Caille et al. 1998). The signal(s) causing the cells to orient, and possibly lengthen, may arise from as little as a single stretch or as a result of multiple stretches.

In summary, a stretch device was used as a developmental model to determine the effects of long bone growth on fiber length and orientation of mammalian skeletal muscle. The considerable flexibility of this model lies in the ability to vary the type and magnitude of mechanical stimuli, and in the opportunity it offers to isolate the effect of the mechanical stimulus in cell culture. Mammalian myoblasts differentiated into myotubes in the device. They responded to a continuous stretch by lengthening and aligning along the direction of stretch. This response was strain rate independent within the range of rates tested. To our knowledge, this is the first characterization of cultured mammalian muscle cells in response to a simulation of long bone growth and muscle development. This in vitro model will provide the vehicle needed to study the mechanotransduction mechanisms in many cell types, particularly in skeletal muscle, where these mechanisms are very difficult to study in vivo and where mechanical deformation occurs not only during development, but as a routine part of the cell's contractile activity.

Acknowledgements We would like to thank Eric Spivey and Smita De for their excellent technical assistance.

References

Alway SE, Carson JA, Roman WJ (1995) Adaptation in myosin expression of avian skeletal muscle after weighting and unweighting. J Mus Res Cell Motil 16:111–122

Andersen KL, Norton LA (1991) A device for the application of known simulated orthodontic forces to human cells in vitro. J Biomech 24:649–654

Baldwin K (1996) Effect of spaceflight on the functional, biochemical, and metabolic properties of skeletal muscle. Med Sci Sports Exerc 28:983–987

Belloli DM, Williams JL, Park JY (1991) Calculated strain fields on cell stressing devices employing circular diaphragms as substrates. Trans Orthop Res Soc 16:399

Blau HM, Pavlath GK, Hardeman EC, Chui CP, Silberstein L, Webster SG, Miller SC, Webster C (1985) Plasticity of the differentiated state. Science 230:758–766

Brighton CT, Strafford B, Gross SB, Leatherwood DF, Williams JL, Pollack SR (1991) The proliferative and synthetic response of isolated calvarial bone cells of rats to cyclic biaxial mechanical strain. J Bone Joint Surg 73:320–331

Brownson C, Loughna PT (1996) Alterations in the mRNA levels of two metabolic enzymes in rat skeletal muscle during stretch-induced hypertrophy and disuse atrophy. Pflügers Arch 431:990–992

Buckley MJ, Banes AJ, Levin LG, Sumpio BE, Sato M, Jordan R, Gilbert J, Link GW, Tran Son Tay R (1988) Osteoblasts increase their rate of division and align in response to cyclic, mechanical tension in vitro. Bone Miner 4:225–236

Caille N, Tardy Y, Meister JJ (1998) Assessment of strain field in endothelial cells subjected to uniaxial deformation of their substrate. Ann Biomed Eng 26:409–416

Eisenburg BR, Salmons S (1981) The reorganization of subcellular structure in muscle undergoing fast-to-slow type transformation. Cell Tissue Res 220:449–471

Endo T, Masaki T (1984) Differential expression and distribution of chicken skeletal and smooth-muscle-type a-actinins during myogenesis in culture. J Cell Biol 99:2322–2332

Franzini-Armstrong C, Fischman DA (1994) Morphogenesis of skeletal muscle fibers. In: Engel AG, Franzini-Armstrong C (eds) Myology basic and clinical. McGraw-Hill, New York, pp 74–96

Funanage VL, Smith SM, Minnich MA (1992) Entactin promotes adhesion and long-term maintenance of cultured regenerated skeletal myotubes. J Cell Physiol 150:251–257

Fung YC (1965) Foundations of solid mechanics. Prentice-Hall, Englewood Cliffs, New Jersey

Fung YC (1993) Biomechanics – mechanical properties of living tissues, 2nd edn. Springer, New York

Galler S (1994) Stretch activation of skeletal muscle fibre types. Pflugers Arch 427:384–386

Gans C, Gaunt AS (1991) Muscle architecture in relation to function. J Biomech 24(Suppl 1):53–65

Garrett WE Jr, Best TM (1994) Anatomy, physiology, and mechanics of skeletal muscle. American Academy of Orthopaedic Surgeons, Rosemont, IL

Goldspink G, Scutt A, Martindale J, Jaenicke T, Turay L, Gerlach G-F (1991) Stretch and force generation induce rapid hypertrophy and myosin isoform gene switching in adult skeletal muscle. Biochem Soc Trans 19:368–373

Hartley RS, Yablonka-Reuveni Z (1990) Long-term maintenance of primary myogenic cultures on a reconstituted basement membrane. In Vitro Cell Dev Biol 26:955–961

Ives CL, Eskin SG, McIntire LV (1986) Mechanical effects on endothelial cell morphology: in vitro assessment. In Vitro Cell Dev Biol 22:500–507

Kanda K, Matsuda T (1994) Mechanical stress-induced orientation and ultrastructural change of smooth muscle cells cultured in three-dimensional collagen lattices. Cell Transplant 3:481–492

Lyles JM, Amin W, Weill CL (1992) Matrigel enhances myotube development in a serum-free defined medium. Int J Dev Neurosci 10:59–73

Maley MA, Davies MJ, Grounds MD (1995) Extracellular matrix, growth factors, genetics: their influence on cell proliferation and myotube formation in primary cultures of adult mouse skeletal muscle. Exp Cell Res 219:169–179

Mills I, Cohen CR, Kamal K, Li G, Shin T, Du W, Sumpio BE (1997) Strain activation of bovine aortic smooth muscle: study of strain dependency and the role of protein kinase A and C signalling pathways. J Cell Physiol 170:228–234

Neidlinger-Wilke C, Wilke H-J, Claes L (1994) Cyclic stretching of human osteoblasts affects proliferation and metabolism: a new experimental method and its application. J Orthop Res 12:70–78

Patton LT, Kaufman MH (1995) The timing of ossification of the limb bones, and growth rates of various long bones of the fore and hind limbs of the prenatal and early postnatal laboratory mouse. J Anat 186:175–185

Rastinejad F, Blau HM (1993) Genetic complementation reveals a novel regulatory role for 3' untranslated regions in growth and differentiation. Cell 72:903–917

Russell B, Dix DJ, Haller DL, Jacobs-El J (1992) Repair of injured skeletal muscle: a molecular approach. Med Sci Sports Exerc 24:189–196

Samuel JL, Vandenburgh HH (1990) Mechanically induced orientation of adult rat cardiac myocytes in vitro. In Vitro Cell Dev Biol 26:905–914

Schaffer JL, Rizen M, L'Italien GJ, Benbrahim A, Megerman J, Gerstenfeld LC, Gray ML (1994) Device for the application of a dynamic biaxially uniform and isotropic strain to a flexible cell culture membrane. J Orthop Res 12:709–719

Shirinsky VP, Antonov AS, Birukov KG, Sobolevsky AV, Romanov YA, Kabaeva NV, Antonova GN, Smirnov VN (1989) Mechano-chemical control of human endothelium orientation and size. J Cell Biol 109:331–339

Tabary JC, Tabary C, Tardieu C, Tardieu G, Goldspink G (1972) Physiological and structural changes in the cat's soleus muscle due to immobilization at different lengths by plaster casts. J Physiol 224:231–244

Tagawa H, Rozich JD, Tsutsui H, Narishige T, Kuppuswamy D, Sato H, McDermott PJ, Koide M, Cooper G IV (1996) Basis for increased microtubules in pressure-hypertrophied cardiocytes. Circulation 93:1230–1243

Terracio L, Miller B, Borg TK (1988) Effects of cyclic mechanical stimulation of the cellular components of the heart: in vitro. In Vitro Cell Dev Biol 24:53–58

Torgan CE, Reedy MC, Kraus WE (1996) Isolation, growth and differentiation of adult rabbit skeletal myoblasts in vitro. Methods Cell Sci 18:299–307

Tsutsui H, Tagawa H, Kent RL, McCollam PL, Ishihara K, Nagatsu M, Cooper G (1994) Role of microtubules in contractile dysfunction of hypertrophied cardiocytes. Circulation 90:533–555

Vandenburgh HH (1982) Dynamic mechanical orientation of skeletal myofibers in vitro. Dev Biol 93:438–443

Vandenburgh HH (1988) A computerized mechanical cell stimulator for tissue culture: effects on skeletal muscle organogenesis. In Vitro Cell Dev Biol 24:609–619

Vandenburgh HH, Karlisch P (1989) Longitudinal growth of skeletal myotubes in vitro in a new horizontal mechanical cell stimulator. In Vitro Cell Dev Biol 25:607–616

Vandenburgh HH, Shansky J, Solerssi R, Chromiak J (1995) Mechanical stimulation of skeletal muscle increases prostaglandin F2α production, cyclooxygenase activity, and cell growth by a pertussis toxin sensitive mechanism. J Cell Physiol 163: 285–294

White TP, Esser KA (1989) Satellite cell and growth factor involvement in skeletal muscle growth. Med Sci Sports Exerc 21:S158–S163

Williams P, Watt P, Bicik V, Goldspink G (1986) Effect of stretch combined with electrical stimulation on the type of sarcomeres produced at the ends of muscle fibers. Exp Neurol 93:500–509

Yaffe D, Saxel O (1977) Serial passaging and differentiation of myogenic cells isolated from dystrophic mouse muscle. Nature 270:725–727